NASA TN D-210

TECHNICAL NOTE
D-210

ROTATING-BEAM FATIGUE TESTS OF NOTCHED AND UNNOTCHED 7075-T6 ALUMINUM-ALLOY SPECIMENS UNDER STRESSES OF CONSTANT AND VARYING AMPLITUDES

By Herbert F. Hardrath, Elmer C. Utley, and David E. Guthrie

Langley Research Center
Langley Field, Va.

NATIONAL AERONAUTICS AND SPACE ADMINISTRATION

WASHINGTON December 1959

W

NATIONAL AERONAUTICS AND SPACE ADMINISTRATION

TECHNICAL NOTE D-210

ROTATING-BEAM FATIGUE TESTS OF NOTCHED AND UNNOTCHED 7075-T6 ALUMINUM-ALLOY SPECIMENS UNDER STRESSES OF CONSTANT AND VARYING AMPLITUDES

By Herbert F. Hardrath, Elmer C. Utley,
and David E. Guthrie

SUMMARY

Unnotched and notched rotating-beam specimens made of 7075-T6 aluminum alloy were tested under constant and varying stress amplitude. Static mechanical properties and constant-amplitude fatigue tests of unnotched specimens yielded results higher than average for the material. Fatigue tests of notched specimens indicated the material was more notch sensitive than indicated by other data. Lives obtained in fatigue tests with variable amplitude were generally less than expected on the basis of the linear cumulative damage rule.

INTRODUCTION

The estimation of the expected life of a given part of an aircraft structure depends, among other things, upon considerations of the size and shape of the part, the loading history to which it may be subjected, and the fatigue properties of the material from which it is made. Reliable rules for combining these pieces of information and applying them to a design case are lacking at present. Consequently, many fatigue tests are conducted on actual parts in order to prove the adequacy of the design from the fatigue standpoint.

The Langley Research Center of the National Aeronautics and Space Administration is conducting research intended to provide data which will help to formulate the design rules which are needed before a structure may be evaluated for its fatigue behavior without extensive tests. The present paper presents results of a systematic series of tests conducted on notched and unnotched 7075-T6 aluminum-alloy rotating-beam specimens under constant and variable stress amplitudes. In most cases a given test was repeated 3 to 10 times in order to provide information on scatter. The testing techniques, equipment, data, and elementary analysis are discussed.

SYMBOLS

K_N	Neuber technical stress concentration factor
K_T	theoretical stress concentration factor
n	number of load cycles applied at a given stress level
Δn	increment in number of load cycles applied at a given stress level
N	number of cycles of load required to produce failure
S_{min}	minimum stress amplitude, ksi
S_{max}	maximum stress amplitude, ksi
ΔS	increment in stress amplitude, ksi
ρ	radius of curvature of notch, in.
ρ'	material constant, in.
ω	included angle in notch, radians

SPECIMENS

All test specimens were cut from 40 ten-foot lengths of 7075-T6 extruded aluminum-alloy rod 1/2 inch in diameter. One tensile test specimen and one compressive test specimen were cut from each end of each rod. The tensile test specimens were standard 0.3-inch-diameter specimens prepared according to reference 1. Compressive test specimens were $1\frac{1}{2}$ inches long with ends ground parallel to each other and normal to the axis; the cylindrical surfaces were left as received.

Twenty-five fatigue-test specimen blanks $3\frac{3}{4}$ inches long were cut from each rod. To be consistent with a previously used numbering system, each blank was identified by the letter B to represent 7075-T6 aluminum alloy, a number between 1 and 40 to identify the rod from which the blank was cut, the letter F for fatigue specimen, and a number between 1 and 25 to identify the location of each specimen within the rod from which it was cut.

Unnotched fatigue specimens were machined to the dimensions shown in figure 1. The procedures used for machining unnotched specimens were identical with those used for preparing 2024-T4 specimens in reference 2. Briefly, machining was in several steps, each step removing less material than the preceding step. In order to assure that light cuts were taken, all machining was done with the specimens mounted on lathe centers with no torque-transferring device except the friction on these centers. Polishing was done in a superfinishing machine in five steps, each at right angles to the previous step. The last two polishing steps used 0.5-micron chromic oxide polishing agent suspended in mineral oil applied in metallurgical polishing broadcloth. The final step was in the longitudinal direction and produced a surface which was expected to be reasonably free of work hardening. The quality of finish was approximately the same as that of the 2024-T4 specimens tested in reference 2. (The estimated surface profile was 2 to 4 microinches root mean square.)

To cover a range of notch severities, notched specimens with three different root radii were prepared according to the dimensions shown in figure 1. The specimens with 0.094-inch radius were machined with a 3/16-inch-diameter milling tool rotated about an axis perpendicular to the axis of the specimen. (See fig. 2.) Manual feed was used and the tool was removed before it began to chatter. A uniformly smooth surface with final tool marks in the longitudinal direction was obtained. Polishing was done in two steps with 0.5-micron chromic oxide on a cord made up of several plies of knitting yarn. In the first step the yarn was rotated very slowly by hand while the specimen was rotated at about 260 revolutions per minute. In the second step the yarn was rotated by a motor at several hundred revolutions per minute while the specimen rotated at 25 revolutions per minute. Both operations were done with the aid of the apparatus shown in figure 3.

The specimens with 0.010-inch and 0.0032-inch root radii were machined in a lathe by using a carefully ground tool. Polishing was similar to that for specimens with 0.094-inch radius except that cotton threads were used and smaller weights were applied.

Each specimen was examined for surface irregularities and was used only if the surface was free of scratches, voids, and so forth. Diameters were measured and the notch radii were checked in a toolmaker's microscope.

TESTING EQUIPMENT

Fatigue specimens were tested in 9 conventional 200-inch-pound capacity R.R. Moore rotating-beam fatigue-testing machines operating at 8,000 revolutions per minute. Three of these machines were equipped with special loading devices which varied the applied load continuously for variable-amplitude tests.

Two of the loading units were modified versions of units used for tests reported in reference 2. These units are shown schematically in figure 4(a). The device is simply a cam-driven lever B which pivots at a fulcrum F and stretches a calibrated spring S attached to the loading yoke of the machine. The cam drive derives its power through gear boxes G_1 and G_2 from the motor M which turns the specimen A to insure positive synchronization between cam and specimen. This feature is the only significant change made to this equipment since it was used for the tests reported in reference 2. Adjustment of the position of the pivot on the beam produced different displacements in the spring for a given displacement of the cam. The adjustment of the turnbuckle T introduced an initial load in the system. Both adjustments were made to select various combinations of minimum and maximum load and consequently minimum and maximum stress amplitudes. Counterweights W were attached to each housing to allow application of low stresses. Dial gage D was used to measure spring deflections.

Two different cams C were used to provide two loading spectra: cam A produced stress amplitudes which were modulated sinusoidally with time and cam B produced stress amplitudes modulated according to an exponential function. Figure 5 presents typical time histories of stresses produced by each of these cams. Departure from the exponential function of cam B occurred at high stresses because a follower with a 1/2-inch radius was used in the lever. Thus, the sharp point on the cam was effectively rounded off. Although the cam speed was adjustable with respect to the speed of the specimen in several steps, all tests were conducted with the cam making one revolution for each 10,000 revolutions of the specimen.

The third loading device, shown schematically in figure 4(b), was designed to apply stresses according to the gust-frequency spectrum. (See ref. 3.) The main features which make this system different from the one just described are: (1) the load comes from a poise P rolling along a pivoted track, (2) the cam C is shaped to apply maximum force when the cam radius is a minimum to eliminate rounding off the sharp point even though a follower of finite radius was used, (3) the entire machine stops each time the cam makes one complete revolution instead of operating continuously, and (4) another gear box G_3 with 1:1 and 10:1 gear ratios is mounted between the motor and specimen housings.

Since the cumulative gust-frequency spectrum (ref. 3) is essentially a straight line extending over several log cycles when plotted on semilog paper, it is impossible to represent the complete spectrum on a cam of reasonable size. In order to overcome this difficulty, the cam was designed to reproduce a segment of the complete curve and successive segments were used to represent the entire spectrum in each test. After one cam revolution, the machine stopped, the relative speed of specimen and cam was changed by a factor of 10, the weight hanging directly below the loading yoke was changed, and the machine restarted. These adjustments were made after each cam revolution until the entire spectrum was applied and then the entire process was repeated until failure occurred. Figure 6 illustrates the gust-frequency spectrum and a typical cumulative frequency spectrum applied during one complete program in the present tests. Segment A was applied by rotating the cam once for 10^5 revolutions of the specimen while the stress amplitude in the specimen varied between 2 and 10 ksi. Segment B was applied by rotating the cam once for 10^4 revolutions of the specimen while the stress amplitude varied between 10 and 18 ksi, and so forth. The ratio 1,000:1 between specimen speed and cam speed was obtained by reducing the rotational speed of the specimen by a factor of 10 at gear box G_3 (shown in fig. 4(b)). A solenoid release mechanism L was provided to remove the load when the power to the motor was interrupted. This device prevented application of unwanted transient stresses while the motor coasted to a stop.

For comparison, the cumulative frequency diagrams for the three stress spectra used are given in figure 7.

TESTS

Tensile and compressive tests were performed to obtain stress-strain curves for 80 tensile specimens and 80 compressive specimens. Ultimate tensile strength and elongation in a 1-inch gage length were also measured on tensile specimens. Strains were measured with electromagnetic extensometers having a 1-inch gage length for tensile tests and a 1/2-inch gage length for compressive tests.

Since all tests were conducted in rotating-beam fatigue testing machines, stresses were completely reversed in all tests. Constant-amplitude fatigue tests were conducted on specimens with each of the shapes shown in figure 1. Testing was done in the usual manner in the six units not equipped for variable-amplitude loading. However, in order to remove bias which might be introduced by a given machine, 10 sets of spindle housings were used, and each housing was used on 1 of the 10 tests performed at a given stress level on a given specimen configuration. Tests were conducted in the machine base that was available

at the start of a given test. Since the machine base has no moving parts except in the motor, no bias was expected from the fact that the machine bases were not systematically rotated in the test schedule. A random sequence of testing was used to eliminate time-dependent effects such as machine wear, specimen aging, and so forth. An exception to this rule occurred for notched specimens with 0.010-inch radius tested at 30 and 36 ksi. These stress levels were not planned in the original program and were, therefore, conducted at the end of the schedule, all within a few days.

Fatigue tests conducted with varying stress amplitudes were conducted on unnotched and 0.010-inch-radius notched specimens only. The same 10 spindle housings used for constant-amplitude tests were used in random sequence. Tests using cams producing sinusoidal or exponential distributions of stress amplitudes were started at the highest stress amplitude in the schedule. Since the increment in load applied to the specimen was fixed and slight variation in specimen diameters was present, the minimum stress amplitude in a given group of tests varied somewhat.

Tests with the gust-frequency spectrum were started at the lowest stress in each increment to minimize errors in loading which might occur if tests were started and stopped when the rate of change in stress was greatest. The weight of the carriage and the stationary weight were adjusted for each specimen; thus all tests in a given group were conducted at the same stress levels. In order to provide a variety of test conditions with the same loading device, the spectrum produced by the machine was modified arbitrarily. In the basic schedule the minimum stress amplitude applied was 2 ksi and each revolution of the cam produced an increment of 8 ksi to a maximum of 34 ksi. In another schedule, the first stress increment was omitted so that stress amplitudes varied between 10 ksi and 34 ksi. A third schedule was arranged to produce a stress increment of 5 ksi for each cam revolution. The minimum stress amplitude was 9 ksi and the maximum was 29 ksi. This change altered the slope of the gust-frequency curve, shown in figure 7, to 5/8 of the slope shown. The test condition would correspond to a design condition using a higher design load factor.

The alinement of each specimen-bearing housing assembly was checked with dial gage indicators. Specimens were not used if the eccentricity of the assembly was greater than 0.0015 inch.

RESULTS AND DISCUSSION

Mechanical Properties

The mechanical properties obtained in tension and compression tests are listed in table 1(a). Each value in the table is the average of 80 test results. The yield stresses and ultimate tensile strengths are considerably higher than specification values listed in reference 4.

A 12-inch-long piece of one of the rods was submitted to the Alcoa Research Laboratories (ARL) to verify the results. Mechanical properties and results of a chemical analysis performed by the ARL are listed in table 1(b). The mechanical properties are seen to be in good agreement with NASA values and the chemical analysis indicates satisfactory composition. Thus, the chemical composition of the material was within specification limits for 7075-T6 aluminum-alloy rod but the properties were somewhat better than average.

Constant-Amplitude Fatigue Tests

The results of fatigue tests at constant stress amplitude are listed in table II. The corresponding S-N curves are presented in figure 8 for unnotched specimens and for specimens with 0.010-inch notch radius and in figure 9 for specimens with 0.094-inch and 0.0032-inch notch radius. The symbols in each figure represent the median of the numbers of cycles to failure for each group of specimens tested under identical conditions. The extent of scatter in life for each group is indicated by the ticks. The median values were chosen to represent each group of data because this is the simplest quantity which can be used in situations where some specimens fail and others do not.

The scatter for unnotched specimens is seen to be considerably greater than was found for 2024-T4 unnotched specimens tested in reference 2. However, the results fall within the scatter band presented for 7075-T6 unnotched rotating beams in reference 4. For comparison, the dashed curve in figure 8 represents the average curve for data in reference 4. The present results are generally above this curve. The run-out stress, that is, the stress at which there is a 50-percent probability of failure in 5×10^8 cycles, is approximately 24 ksi for unnotched specimens and 20 ksi, 9.6 ksi, and 6.3 ksi for notched specimens in order of increasing notch severity.

The scatter in results for tests of notched specimens (figs. 8 and 9) is about as great as that for unnotched specimens. The dashed curves drawn near the data for notched specimens with 0.010-inch and 0.0032-inch radii are the average curves given in reference 4 for rotating beam tests

of 7075-T6 aluminum-alloy specimens having notches with approximately 0.0002-inch radius.

The average curve for the present data for notches with 0.010-inch radius is very close to the dashed curve and the average of present data for notches with 0.0032-inch radius is well below the curve. Thus, the present material has somewhat greater than average fatigue strength in the unnotched specimens, but its notch sensitivity appears to be enough greater than average to produce lower than average fatigue strength in notched specimens.

The dot-dash curves in figures 8 and 9 are predictions of fatigue behavior made by a modified form of the Neuber technical stress concentration factor K_N. (See ref. 5.) The original Neuber equation is:

$$K_N = 1 + \frac{K_T - 1}{1 + \frac{\pi}{\pi - \omega}\sqrt{\frac{\rho'}{\rho}}} \qquad (1)$$

Later research (refs. 6 and 7) has shown that the influence of the included angle in the notch is considerably less, for angles in the range 0° to 90°, than that predicted by the Neuber formula. Equation (1) was, therefore, modified to the form $K_N = 1 + \frac{K_T - 1}{1 + \sqrt{\frac{\rho'}{\rho}}}$ to eliminate the effect of notch angle for these calculations. The material constant ρ' was adjusted empirically to a value of 0.002 inch to produce the best fit with the present data. The elastic stress concentration factors K_T for the notched configurations tested were 1.38, 3.0, and 5.0 for notch radii of 0.094, 0.010, and 0.0032 inch, respectively. The corresponding Neuber factors were 1.33, 2.37, and 3.23, respectively. The prediction made in this manner is lower than that for the data for specimens with the mildest notch but is very good for specimens with the two sharper notches.

Variable-Amplitude Tests

The results of individual tests in which the stress amplitude varied are listed in table III. The test results are grouped by specimen configuration and loading spectrum in parts (a) to (d) of the table. Within

each part of the table, the results are grouped by the maximum stress amplitude S_{max} and by the increment in stress amplitude ΔS. As indicated earlier, the increment in stress amplitude varied because of variations in specimen diameter. The resulting minimum stresses are given for each specimen and the value of ΔS for each group is approximate. The median life for each group of tests is also listed in the table.

The results of tests conducted with the gust-frequency spectrum are listed in table III(e). These tests are grouped by minimum stress in the spectrum and the increment in stress obtained in one revolution of the cam.

The data have been analyzed according to the linear cumulative damage hypothesis. For the tests with sinusoidal and exponential stress modulation, the life of each specimen was divided into 12 equal increments Δn. The arithmetic mean of the maximum and minimum stresses for each of the stress increments was used to determine N, the number of cycles of load required to produce failure in a constant-level test at each stress increment. A value of $\Delta n/N$ was obtained for each increment and these were added to obtain $\sum \frac{n}{N}$ for each test. The details of this computation are described more completely in reference 2. Values of $\sum \frac{n}{N}$ and the median of these values within each group of tests are also listed in table III. Figures 10 to 12 present the results in graphic form. Data for unnotched specimens tested under sinusoidally and exponentially varying loading spectra are presented in figure 10. Similar data for notched specimens are presented in figure 11 and data for notched specimens tested with the gust-frequency spectrum are given in figure 12. The logarithmic scale was chosen for $\sum \frac{n}{N}$ because this quantity is a measure of life of specimens and fatigue lives are conventionally plotted on a log scale. The symbols represent the median of $\sum \frac{n}{N}$ for each group and the scatter is indicated by the ticks. The percentage scatter in $\sum \frac{n}{N}$ should be expected to be about as great as that in the lives of specimens loaded at constant amplitude. Most of the present tests involved stresses near the run-out stress where the scatter is usually greatest in constant-level tests. Thus, the scatter in $\sum \frac{n}{N}$ shown is not surprising.

In general, the number of tests in each group is too small to permit a critical assessment of scatter, but results of tests for notched specimens were subject to less scatter than were unnotched specimens tested under similar loading conditions. There is also some indication that scatter increased as the maximum stress decreased. The scatter in results of tests using the gust-frequency spectrum was surprisingly small.

The median values of $\sum \frac{n}{N}$ were less than 1.0 for all groups of tests on notched specimens. Median values of $\sum \frac{n}{N}$ for unnotched specimens were less than 1.0 in 12 of the 18 cases. On the whole, this observation is in agreement with results of other tests of rotating-beam specimens tested with stresses varying in amplitude. A contributing factor for the occurrence of failure when $\sum \frac{n}{N}$ is less than 1 is probably the damage caused by stresses below the run-out stress after cracks form. (See ref. 8.) Fatigue cracks cause higher stress concentrations than were present previously; thus, the minimum stress for which damage is to be expected is decreased. Such damage is, of course, not evaluated in the calculation of $\sum \frac{n}{N}$.

Inspection of figures 10 and 11 reveals no systematic variation in $\sum \frac{n}{N}$ with stress level or shape of spectrum. This condition is in contrast to what appeared to be a systematic variation in $\sum \frac{n}{N}$ with shape of spectrum observed in reference 2. It is possible that the effect noted in reference 2 was the result of a potential variation in the speed with which the specimen was driven while a separate motor drove the cam-lever system at essentially constant speed. The speed of the testing machine is somewhat slower when the load on the specimen is high. This speed change was probably greater for the sinusoidal cam than for the exponential cam because more time was spent at high loads and more of the inertia in the system was dissipated before the speed again increased. Slowing down the specimen while the load applied to the housings is high resulted in fewer than the proper number of cycles at high stress. Since this variation in speed was not evaluated, it could not be accounted for in the analysis of the results. Thus, the computed

value of $\sum \frac{n}{N}$ was higher than it would have been if the effects of speed change on the stress spectrum had been known. The synchronized loading apparatus introduced in the present tests assured that the desired loading was applied and this condition seems to have eliminated the apparent effect of spectrum shape which was noted in reference 2.

The scatter in results of tests with the gust-frequency spectrum was surprisingly small. The mean values of $\sum \frac{n}{N}$ for the three groups of tests were also grouped closely about a value of approximately 0.4.

CONCLUDING REMARKS

Static tests and fatigue tests with constant and varying stress amplitudes have been conducted on 7075-T6 extruded aluminum-alloy bar stock. The static tensile and compressive properties were found to be substantially higher than specification values for this alloy. Results of constant-amplitude fatigue tests of unnotched specimens were subject to considerable scatter but in general were higher than mean values of data presented previously. Results of constant-level fatigue tests of notched specimens indicated somewhat higher notch sensitivity than was expected on the basis of previous information. Results of variable-amplitude fatigue tests of unnotched and notched specimens were analyzed according to the linear cumulative damage hypothesis. The values of the summation of cycle ratios $\sum \frac{n}{N}$ thus obtained tended to be less than 1 and did not appear to be affected by the shape of spectrum used. The scatter in life under variable-amplitude stresses was of the same order as that under constant-amplitude stressing.

Langley Research Center,
National Aeronautics and Space Administration,
Langley Field, Va., October 6, 1959.

REFERENCES

1. Anon.: Standard Methods of Tension Testing of Metallic Materials. A.S.T.M. Designation: E 8-46. Pt. 1 of 1949 Book of A.S.T.M. Standards Including Tentatives. A.S.T.M. (Philadelphia), 1950, pp. 1233-1244.

2. Hardrath, Herbert F., and Utley, Elmer D., Jr.: An Experimental Investigation of the Behavior of 24S-T4 Aluminum Alloy Subjected to Repeated Stresses of Constant and Varying Amplitudes. NACA TN 2798, 1952.

3. Rhode, Richard V., and Donely, Philip: Frequency of Occurrence of Atmospheric Gusts and of Related Loads on Airplane Structures. NACA WR L-121, 1944. (Formerly NACA ARR L4I21.)

4. Anon.: Strength of Metal Aircraft Elements. ANC-5 Bull., Rev. ed., Depts. of Air Force, Navy, and Commerce, Mar. 1955.

5. Neuber, H.: Theory of Notch Stresses: Principles for Exact Stress Calculation. Translation 74, The David W. Taylor Model Basin, U.S. Navy, Nov. 1945.

6. Leven, M. M., and Frocht, M. M.: Stress-Concentration Factors for Single Notch in Flat Bar in Pure and Central Bending. Jour. Appl. Mech., vol. 19, no. 4, Dec. 1952, pp. 560-561.

7. Neuber, H.: Kerbspannungslehre. Second ed., Springer-Verlag (Berlin/Göttingen/Heidelberg), 1958.

8. Anon.: Discussion in New York by Herbert F. Hardrath (Langley Field, Va.). Proc. Int. Conf. on Fatigue of Metals (London and New York), Inst. Mech. Eng. and A.S.M.E., 1956, p. 830.

TABLE I.- MECHANICAL PROPERTIES

(a) NASA results

	Tension	Compression
Yield stress (0.2 percent offset), ksi:		
Maximum	96.3	93.5
Minimum	88.4	87.4
Average	92.7	90.6
Ultimate strength, ksi:		
Maximum	100.6	----
Minimum	94.5	----
Average	98.0	----
Elongation in 1-inch gage length, percent:		
Maximum	16	----
Minimum	8	----
Average	12	----

(b) ARL results

Ultimate tensile strength, ksi	98.5
Yield stress (0.2 percent offset), ksi	93.6
Elongation, percent	9.6
Chemical analysis, percent:	
Cu	1.65
Fe	0.23
Si	0.11
Mn	0.02
Mg	2.63
Zn	6.09
Cr	0.22
Ti	0.03

TABLE II.- RESULTS OF CONSTANT-AMPLITUDE ROTATING-BEAM FATIGUE TESTS OF 7075-T6 ALUMINUM ALLOY

(a) Unnotched specimens

Specimen	Cycles to failure	Specimen	Cycles to failure
S = 45 ksi		S = 36 ksi	
B2F10	369,000	B6F13	929,000
B32F11	209,000	B11F10	763,000
B13F6	190,000	B10F7	430,000
B17F6	186,000	B39F14	401,000
B20F13	134,000	B28F13	314,000
B6F7	105,000	B5F7	298,000
B25F11	103,000	B11F7	266,000
B17F8	76,000	B9F13	219,000
B12F4	75,000	B31F8	208,000
		B40F7	179,000
Median	134,000	Median	306,000
S = 32 ksi		S = 28 ksi	
B29F11	3,844,000	B17F4	42,229,000
B35F11	2,993,000	B5F13	26,681,000
B40F8	776,000	B24F14	18,223,000
B7F4	776,000	B34F8	7,449,000
B24F7	665,000	B34F13	6,902,000
B37F14	665,000	B10F6	3,005,000
B16F8	600,000	B31F4	1,876,000
B27F13	504,000	B4F8	1,738,000
B19F8	374,000	B17F10	979,000
B26F17	319,000	B4F7	902,000
Median	665,000	Median	4,953,500
S = 26 ksi		S = 25 ksi	
B39F4	>549,810,000	B23F11	>509,037,000
B18F7	278,328,000	B2F13	291,754,000
B3F10	222,182,000	B17F7	243,666,000
B18F13	135,577,000	B33F8	186,662,000
B8F6	122,367,000	B37F7	85,167,000
B32F8	65,317,000	B19F17	63,380,000
B14F17	40,055,000	B10F10	57,408,000
B14F13	38,539,000	B4F14	27,358,000
B8F17	11,419,000	B36F4	25,108,000
B10F8	1,004,000	B18F6	16,089,000
		B10F4	2,590,000
Median	93,842,000	Median	63,380,000
S = 24 ksi		S = 23 ksi	
B36F17	>517,318,000	B6F4	>863,224,000
B16F10	>510,055,000	B7F10	>590,857,000
B22F7	>506,378,000	B18F10	>547,322,000
B4F10	>504,590,000	B15F10	>544,945,000
B16F14	104,613,000	B21F4	>530,763,000
B1F13	8,161,000	B24F13	>516,099,000
B13F17	4,090,000	B20F6	>505,082,000
B10F17	3,456,000	B18F17	205,282,000
B9F8	2,408,000	B25F17	137,207,000
B11F13	2,310,000		
Median	56,387,000	Median	>530,000,000
S = 22 ksi			
B38F13	>995,264,000		
B27F11	>764,156,000		
B16F13	380,494,000		
Median	>764,156,000		

TABLE II.- RESULTS OF CONSTANT-AMPLITUDE ROTATING-BEAM FATIGUE TESTS OF 7075-T6 ALUMINUM ALLOY - Continued

(b) 0.094-inch radius

Specimen	Cycles to failure	Specimen	Cycles to failure
S = 36 ksi		S = 32 ksi	
B3F3	3,318,000	B27F3	11,600,000
B25F3	282,000	B33F3	721,000
B38F3	144,000	B21F19	349,000
B31F3	142,000	B27F19	296,000
B24F10	108,000	B33F19	229,000
B16F20	86,000	B40F10	207,000
B40F19	81,000	B29F3	131,000
B4F20	80,000	B25F19	131,000
B31F10	76,000	B26F10	94,000
B37F10	70,000	B5F20	82,000
Median	97,000	Median	218,000
S = 28 ksi		S = 25 ksi	
B36F10	22,918,000	B39F10	32,273,000
B3F20	12,838,000	B34F3	27,558,000
B13F20	4,694,000	B30F10	23,875,000
B37F3	4,611,000	B36F3	19,132,000
B39F3	1,515,000	B33F10	18,995,000
B23F19	1,388,000	B22F10	15,223,000
B30F3	967,000	B24F3	12,560,000
B37F19	766,000	B2F3	11,924,000
B29F10	375,000	B24F19	11,785,000
B28F10	340,000	B36F19	11,348,000
Median	1,451,500	Median	17,109,000
S = 22 ksi		S = 20 ksi	
B32F19	150,412,000	B21F10	>658,449,000
B39F19	118,263,000	B35F19	599,517,000
B26F19	107,573,000	B27F10	>592,748,000
B32F10	88,493,000	B35F10	>512,303,000
B1F3	61,015,000	B21F3	>501,931,000
B26F3	60,528,000	B22F19	309,694,000
B15F20	18,389,000	B28F3	278,180,000
B12F20	7,020,000	B28F19	29,402,000
B25F10	2,571,000	B11F20	9,888,000
Median	61,015,000	Median	>501,931,000

TABLE II.- RESULTS OF CONSTANT-AMPLITUDE ROTATING-BEAM FATIGUE

TESTS OF 7075-T6 ALUMINUM ALLOY - Continued

(c) 0.010-inch radius specimens

Specimen	Cycles to failure	Specimen	Cycles to failure
S = 36 ksi		S = 30 ksi	
B40F21	9,900	B7F18	19,200
B31F21	9,600	B14F12	17,700
B7F21	9,400	B13F12	17,600
B10F21	9,000	B10F18	17,100
B34F21	8,700	B9F18	16,400
B17F15	8,400	B20F12	16,300
B20F15	8,000	B12F12	16,100
B30F21	7,800	B11F12	16,000
B19F15	7,400	B17F12	15,900
B33F21	7,100	B18F12	15,400
Median	8,550	Median	16,350
S = 22 ksi		S = 18 ksi	
B5F2	269,000	B20F24	18,499,000
B19F12	67,000	B30F2	1,916,000
B29F21	63,000	B38F1	877,000
B17F18	59,000	B37F12	642,000
B11F15	57,000	B39F18	592,000
B7F2	52,000	B27F5	480,000
B38F2	51,000	B32F5	446,000
B24F18	46,000	B22F21	205,000
B39F5	44,000	B17F9	171,000
B29F9	40,000	B30F24	121,000
Median	54,500	Median	536,000
S = 16 ksi		S = 13 ksi	
B25F12	763,000	B22F12	6,274,000
B6F15	739,000	B32F21	3,732,000
B11F5	722,000	B10F2	2,422,000
B38F9	643,000	B20F18	2,212,000
B35F21	423,000	B9F9	1,880,000
B23F1	405,000	B27F18	1,565,000
B21F24	303,000	B5F24	1,552,000
B15F2	210,000	B15F24	1,122,000
B30F18	182,000	B24F21	1,107,000
B5F9	41,000	B37F24	1,051,000
Median	414,000	Median	1,722,500
S = 12 ksi		S = 11 ksi	
B40F5	71,645,000	B33F18	268,102,000
B16F15	13,434,000	B14F24	240,710,000
B15F12	12,840,000	B1F12	108,446,000
B34F2	9,625,000	B8F9	63,237,000
B26F21	3,074,000	B29F1	49,208,000
B14F18	3,033,000	B28F12	48,090,000
B28F21	2,429,000	B24F24	11,440,000
B36F24	1,772,000	B16F2	4,938,000
B11F2	1,296,000	B26F12	1,380,000
B9F12	1,289,000	Median	49,208,000
Median	3,053,500		
S = 10 ksi		S = 9 ksi	
B26F1	>515,286,000	B10F12	>1,181,557,000
B17F24	488,868,000	B30F5	>827,652,000
B14F9	486,409,000	B23F21	>733,298,000
B3F12	432,442,000	B23F9	>698,649,000
B29F18	364,450,000	B4F2	>529,500,000
B27F2	354,455,000	B13F24	>509,324,000
B31F12	240,908,000	B31F5	>504,416,000
B4F18	118,135,000	B6F12	>501,046,000
B4F12	108,395,000	B6F21	>500,128,000
B28F24	11,703,000	Median	>529,500,000
Median	359,452,500		

TABLE II.- RESULTS OF CONSTANT-AMPLITUDE ROTATING-BEAM FATIGUE TESTS OF 7075-T6 ALUMINUM ALLOY - Concluded

(d) 0.0032-inch radius specimens

Specimen	Cycles to failure	Specimen	Cycles to failure
S = 22 ksi		S = 18 ksi	
B36F15	41,000	B14F19	689,000
B38F20	36,000	B23F20	445,000
B27F15	36,000	B39F6	399,000
B25F6	36,000	B37F20	71,000
B21F20	33,000	B5F19	52,000
B7F19	29,000	B23F15	47,000
B4F11	28,000	B33F20	44,000
B27F20	20,000	B21F6	36,000
B15F19	17,000	B38F15	31,000
B18F19	17,000	B28F20	29,000
Median	31,000	Median	49,500
S = 13 ksi		S = 10 ksi	
B29F6	842,000	B14F11	1,388,000
B22F15	782,000	B26F15	1,383,000
B33F6	708,000	B24F6	1,276,000
B40F15	690,000	B8F19	1,156,000
B7F11	641,000	B17F19	1,020,000
B13F19	423,000	B36F20	984,000
B31F15	328,000	B3F11	867,000
B32F20	263,000	B34F6	846,000
B4F19	253,000	B35F15	840,000
B22F20	224,000	B26F20	799,000
Median	532,000	Median	1,002,000
S = 9 ksi		S = 8 ksi	
B36F6	2,449,000	B2F11	>1,158,980,000
B12F19	1,766,000	B32F6	33,530,000
B22F6	1,490,000	B1F19	32,072,000
B40F20	1,479,000	B24F15	8,755,000
B30F15	1,445,000	B35F20	5,439,000
B39F20	1,439,000	B23F6	2,845,000
B39F15	1,430,000	B34F15	2,249,000
B3F19	1,132,000	B25F20	2,045,000
B11F19	1,116,000	B16F19	1,668,000
B30F6	735,000	B13F11	1,658,000
Median	1,442,000	Median	4,142,000
S = 7.5 ksi		S = 7 ksi	
B28F15	>787,812,000	B6F19	>1,125,295,000
B26F6	>515,239,000	B33F15	>715,839,000
B28F6	>504,823,000	B24F20	>616,445,000
B27F6	>503,136,000	B35F6	505,327,000
B29F20	122,585,000	B40F6	267,124,000
B2F19	17,774,000	B31F20	197,869,000
B9F11	13,089,000	B34F20	34,984,000
B20F19	11,485,000	B32F15	5,764,000
B1F11	3,682,000	B5F11	2,965,000
B10F19	3,611,000	B15F11	2,758,000
Median	70,179,500	Median	232,496,500

TABLE III.- RESULTS OF VARYING-AMPLITUDE ROTATING-BEAM FATIGUE TESTS OF 7075-T6 ALUMINUM ALLOY

(a) Unnotched specimens; sinusoidal modulation

Specimen	S_{min}, ksi	Cycles to failure	$\sum \frac{n}{N}$
S_{max} = 35 ksi; ΔS = 18 ksi			
B12F6	16.4	3,643,000	2.27
B34F17	15.4	1,809,000	1.11
B3F8	14.8	1,748,000	1.06
B39F13	15.7	1,249,000	.77
B36F13	15.8	1,160,000	.72
B22F13	15.8	1,034,000	.64
B26F14	16.2	1,021,000	.64
B28F17	15.9	888,000	.55
B13F8	15.0	803,000	.49
B3F17	15.1	491,000	.30
B7F17	15.8	490,000	.30
Median		1,034,000	.64
S_{max} = 32 ksi; ΔS = 18 ksi			
B33F7	12.8	34,908,000	8.41
B33F4	12.5	22,652,000	5.42
B24F17	12.1	8,070,000	1.91
B33F13	12.5	4,632,000	1.11
B38F4	12.4	2,430,000	.58
Median		8,070,000	1.91
S_{max} = 31 ksi; ΔS = 18 ksi			
B32F4	11.8	10,121,000	1.59
B2F7	11.9	3,410,000	.54
B11F8	10.6	1,525,000	.24
B11F17	11.1	1,194,000	.19
Median		2,467,500	.39
S_{max} = 30 ksi; ΔS = 18 ksi			
B38F17	10.0	>405,467,000	
B8F10	11.2	64,256,000	6.29
B32F13	10.2	45,500,000	4.30
B3F7	10.7	3,058,000	.29
B16F17*	8.7	2,230,000	.11
B9F17	10.0	1,364,000	.13
B12F17	9.5	1,265,000	.10
Median		3,058,000	.29

*Maximum stress of 29 ksi.

TABLE III.- RESULTS OF VARYING-AMPLITUDE ROTATING-BEAM FATIGUE TESTS OF 7075-T6 ALUMINUM ALLOY - Continued

(a) Unnotched specimens; sinusoidal modulation - Concluded

Specimen	S_{min}, ksi	Cycles to failure	$\sum \frac{n}{N}$
S_{max} = 28 ksi; ΔS = 18 ksi			
B23F14	9.1	96,170,000	2.41
B9F14	9.0	90,444,000	1.92
Median		93,307,000	2.16
S_{max} = 35 ksi; ΔS = 12 ksi			
B33F11	22.8	21,925,000	17.58
B19F7	22.4	20,594,000	16.25
B26F11	22.6	4,944,000	3.94
B19F10	22.0	3,821,000	2.95
B37F11	22.7	1,866,000	1.49
Median		4,944,000	3.94
S_{max} = 30 ksi; ΔS = 12 ksi			
B39F11	17.9	94,420,000	11.90
B20F10	17.4	58,277,000	7.11
B30F11	18.0	51,282,000	6.46
B9F4	17.8	1,433,000	.18
B5F17	18.0	540,000	.07
Median		51,282,000	6.46
S_{max} = 35 ksi; ΔS = 6 ksi			
B19F4	28.2	1,293,000	1.55
B15F6	28.3	606,000	.73
B5F4	28.4	574,000	.70
B33F14	28.2	520,000	.62
Median		590,000	.72
S_{max} = 32 ksi; ΔS = 6 ksi			
B14F7	25.3	2,778,000	1.23
B1F17	25.2	2,718,000	1.20
B15F8	25.1	1,033,000	.45
B23F7	25.1	1,000,000	.44
B29F7	25.2	529,000	.23
Median		1,033,000	.45
S_{max} = 28 ksi; ΔS = 6 ksi			
B32F7	21.3	193,961,000	9.08
B13F10	21.4	78,816,000	3.70
B23F8	21.3	10,640,000	.50
B25F4	21.3	3,065,000	.14
B7F13	21.1	3,060,000	.14
Median		10,640,000	.50

TABLE III.- RESULTS OF VARYING-AMPLITUDE ROTATING-BEAM FATIGUE TESTS OF 7075-T6 ALUMINUM ALLOY - Continued

(b) Unnotched specimens; Exponential modulation

Specimen	S_{min}, ksi	Cycles to failure	$\sum \frac{n}{N}$
S_{max} = 35 ksi; ΔS = 18 ksi			
B15F14	16.4	6,240,000	0.69
B18F4	16.6	5,180,000	.58
B13F13	16.0	2,470,000	.27
Median		5,180,000	.58
S_{max} = 32 ksi; ΔS = 18 ksi			
B38F11	14.1	202,210,000	6.60
B12F10	13.5	175,183,000	5.42
B2F17	13.1	12,780,000	.39
B10F14	13.4	4,591,000	.14
B35F4	13.5	2,909,000	.09
Median		12,780,000	.39
S_{max} = 35 ksi; ΔS = 12 ksi			
B15F13	22.5	3,370,000	0.66
B9F10	22.7	2,501,000	.49
B37F4	22.6	1,773,000	.35
B22F4	22.2	1,325,000	.25
Median		2,137,000	.42
S_{max} = 32 ksi; ΔS = 12 ksi			
B30F17	19.3	108,882,000	5.90
B5F8	19.1	61,080,000	3.28
Median		84,981,000	4.59
S_{max} = 30 ksi; ΔS = 12 ksi			
B2F4	17.9	258,006,000	4.42
B19F13	17.2	237,102,000	3.88
B14F10	18.8	116,334,000	2.15
B35F14	17.7	10,493,000	.18
B20F14	17.6	9,341,000	.16
B1F8	17.1	2,687,000	.04
Median		63,413,000	1.16
S_{max} = 35 ksi; ΔS = 6 ksi			
B4F13	29.0	2,015,000	1.56
B39F8	28.9	1,202,000	.91
B30F14	29.0	1,113,000	.86
Median		1,202,000	.91
S_{max} = 30 ksi; ΔS = 6 ksi			
B9F7	24.2	219,102,000	12.20
B28F4	23.8	4,291,000	.21
B11F14	24.1	666,000	.04
Median		4,291,000	.21
S_{max} = 28 ksi; ΔS = 6 ksi			
B5F14	22.1	146,551,000	1.31
B30F4	21.7	28,194,000	.22
B8F14	22.1	25,138,000	.22
Median		28,194,000	.22

TABLE III.- RESULTS OF VARYING-AMPLITUDE ROTATING-BEAM FATIGUE TESTS OF 7075-T6 ALUMINUM ALLOY - Continued

(c) 0.010-inch radius specimens, sinusoidal modulation

Specimen	S_{min}, ksi	Cycles to failure	$\sum \frac{n}{N}$
S_{max} = 25 ksi; ΔS = 18 ksi			
B22F24	4.4	130,000	1.05
B25F9	4.6	110,000	.90
B26F18	4.2	110,000	.88
B22F18	4.3	109,000	.87
B21F9	4.8	105,000	.86
B36F1	4.5	100,000	.81
B7F5	4.3	91,000	.73
B20F5	4.3	81,000	.65
B31F24	3.9	79,000	.62
Median		105,000	.86
S_{max} = 20 ksi; ΔS = 18 ksi			
B35F18	1.1	1,579,000	3.35
B2F5	1.6	1,452,000	3.11
B34F18	1.4	921,000	1.97
B38F18	2.3	412,000	.90
B24F1	1.6	370,000	.76
B6F18	.8	334,000	.70
B18F18	2.1	234,000	.54
B24F2	1.0	202,000	.43
B33F9	.5	68,000	.14
Median		370,000	.76
S_{max} = 20 ksi; ΔS = 12 ksi			
B12F24	6.4	346,000	0.88
B3F2	6.6	293,000	.75
B24F12	6.6	271,000	.70
B37F2	6.5	271,000	.69
Median		282,000	.72
S_{max} = 18 ksi; ΔS = 12 ksi			
B34F24	4.6	667,000	0.81
B32F12	4.8	594,000	.72
B6F24	5.0	483,000	.60
B17F2	4.9	397,000	.49
B9F2	4.6	304,000	.37
Median		483,000	.60
S_{max} = 20 ksi; ΔS = 6 ksi			
B4F24	12.8	100,000	0.38
B31F9	12.7	100,000	.38
B21F5	12.9	92,000	.35
B28F5	12.8	74,000	.28
Median		96,000	.36
S_{max} = 16 ksi; ΔS = 6 ksi			
B20F9	8.7	609,000	0.43
B22F5	8.9	548,000	.39
B15F2	9.0	497,000	.33
B36F5	9.0	331,000	.24
B27F9	8.7	262,000	.18
Median		497,000	.33
S_{max} = 12 ksi; ΔS = 6 ksi			
B27F1	4.8	21,681,000	0.75
B30F9	4.8	17,741,000	.62
B40F9	4.8	3,733,000	.13
B1F24	4.9	1,200,000	.04
Median		10,737,000	.38
S_{max} = 11 ksi; ΔS = 6 ksi			
B13F9	3.8	394,512,000	2.56
B32F9	3.8	74,000,000	.48
B36F9	3.7	47,911,000	.31
B38F5	3.9	29,279,000	.19
B34F9	3.8	29,101,000	.19
Median		47,911,000	.31

TABLE III.- RESULTS OF VARYING-AMPLITUDE ROTATING-BEAM FATIGUE

TESTS OF 7075-T6 ALUMINUM ALLOY - Continued

(d) 0.010-inch radius specimens, exponential modulation

Specimen	S_{min}, ksi	Cycles to failure	$\sum \frac{n}{N}$
S_{max} = 20 ksi; ΔS = 18 ksi			
B8F12	1.9	3,371,000	1.12
B9F21	.9	1,780,000	.54
B18F2	.38	1,410,000	.42
Median		1,780,000	.54
S_{max} = 20 ksi; ΔS = 12 ksi			
B10F9	6.9	1,050,000	0.55
B2F24	7.0	990,000	.52
B12F9	6.6	978,000	.50
B19F18	6.8	549,000	.29
Median		984,000	.51
S_{max} = 18 ksi; ΔS = 12 ksi			
B25F21	4.6	2,030,000	0.42
B13F18	5.0	1,993,000	.38
B34F2	5.4	1,204,000	.36
Median		1,993,000	.38
S_{max} = 17 ksi; ΔS = 12 ksi			
B2F12	3.7	5,494,000	0.70
B31F18	3.9	4,990,000	.58
B33F1	3.9	4,480,000	.58
Median		4,990,000	.58
S_{max} = 16 ksi; ΔS = 6 ksi			
B37F9	9.5	2,347,000	0.47
B27F12	9.2	1,711,000	.32
B38F12	9.3	1,316,000	.25
B29F5	9.2	879,000	.16
B3F24	9.3	100,000	.02
Median		1,316,000	.25
S_{max} = 14 ksi; ΔS = 6 ksi			
B26F5	7.4	38,000,000	1.59
B34F5	7.7	33,443,000	1.48
B16F9	7.2	6,933,000	.28
B29F12	7.3	4,834,000	.20
B40F12	7.3	2,527,000	.10
Median		6,933,000	.28
S_{max} = 12 ksi; ΔS = 6 ksi			
B39F9	5.4	337,566,000	1.18
B26F9	5.5	255,588,000	.91
B16F24	5.3	153,059,000	.53
B30F12	5.3	44,868,000	.16
B39F12	5.3	42,600,000	.15
Median		153,059,000	.53

TABLE III.- RESULTS OF VARYING-AMPLITUDE ROTATING-BEAM FATIGUE TESTS OF 7075-T6 ALUMINUM ALLOY - Concluded

(e) 0.010-inch radius specimens, gust frequency spectrum

Specimen	Cycles to failure	$\sum \frac{n}{N}$
S_{min} = 2 ksi; ΔS/rev = 8 ksi		
B1F21	2,450,000	0.54
B5F18	2,328,710	.51
B21F12	2,116,700	.48
B6F2	2,019,440	.47
B37F5	2,004,547	.45
B36F12	1,988,780	.45
B29F2	1,906,420	.44
B36F21	1,893,000	.43
B37F21	1,789,600	.41
B39F21	1,781,236	.41
B28F9	1,773,000	.40
B16F18	1,675,620	.39
B23F18	1,668,837	.33
B8F21	1,554,400	.31
Median	1,899,710	.44
S_{min} = 10 ksi; ΔS/rev = 8 ksi		
B4F21	280,115	0.60
B39F1	247,900	.54
B32F2	247,060	.53
B11F9	225,330	.50
B13F5	222,150	.49
B35F2	220,280	.48
B35F9	214,060	.47
B22F2	208,560	.46
B23F5	203,860	.46
B19F9	200,740	.44
B15F9	198,250	.44
B35F24	213,300	.42
B40F1	181,135	.41
B26F24	175,500	.37
B30F1	168,620	.36
Median	208,560	.46
S_{min} = 9 ksi; ΔS/rev = 5 ksi		
B23F12	1,906,720*	0.39
B26F2	1,438,740	.47
B36F18	1,337,930	.46
B7F15	1,326,330	.43
B21F18	1,110,100	.37
B27F21	1,109,730	.37
B13F15	1,106,390	.37
B2F15	968,290	.32
B19F24	865,880	.29
B29F24	743,350	.29
Median	1,109,915	.37

*This test failed before two complete spectra were applied. All other tests were conducted with 1/10 as many cycles per cam revolution.

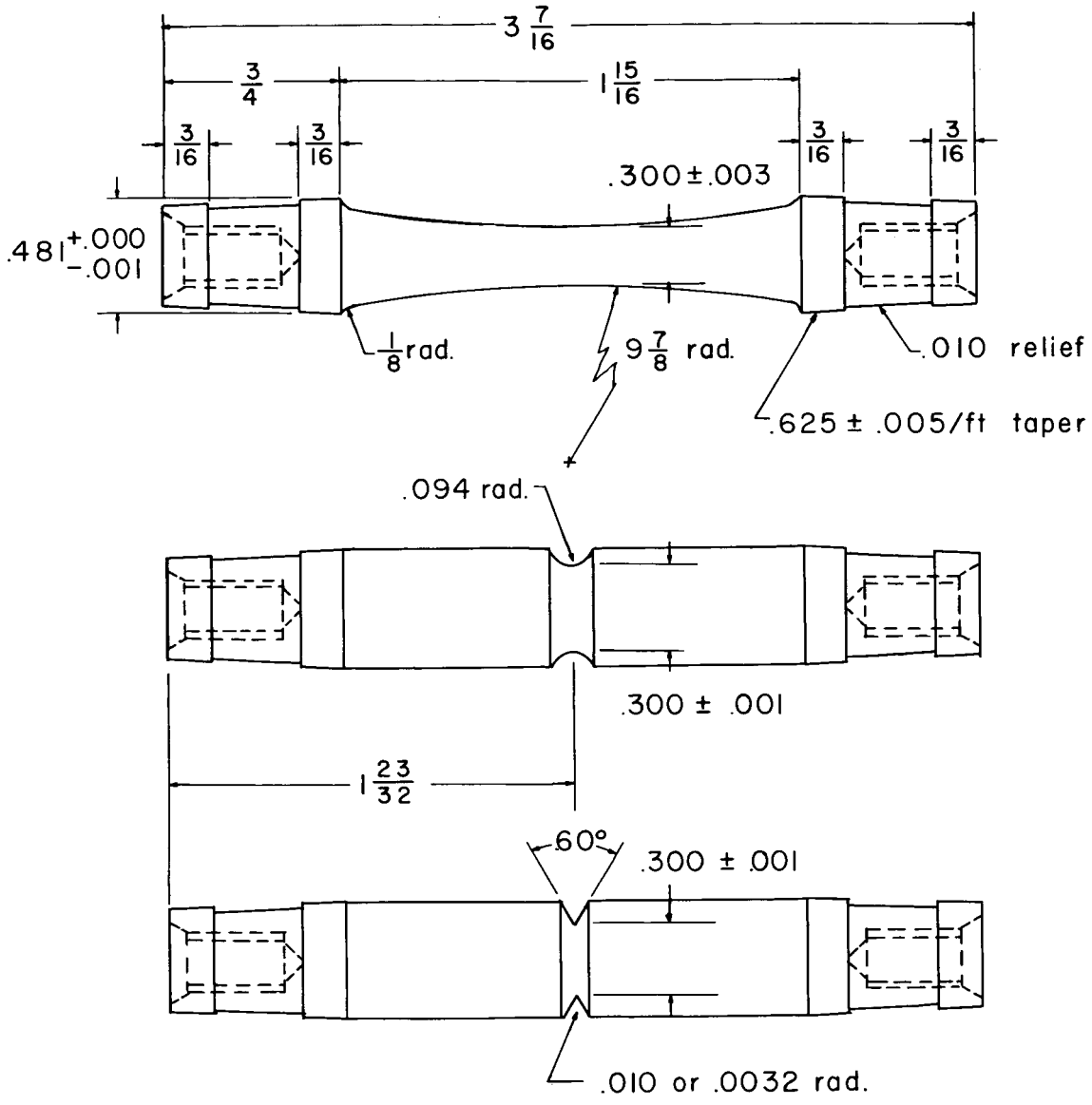

Figure 1.- Specimen configurations. All dimensions are in inches unless otherwise noted.

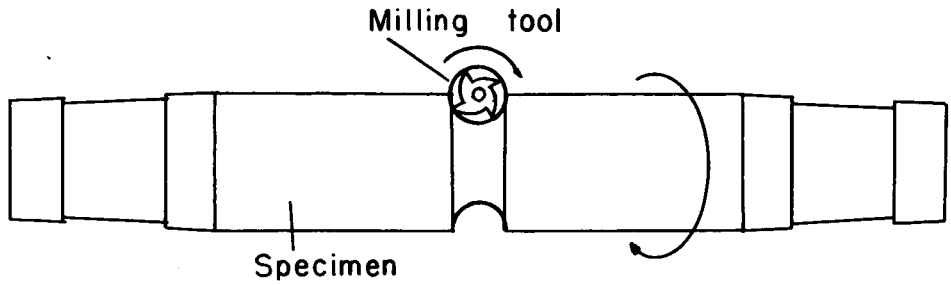

Figure 2.- Machining technique. 0.094-inch radius.

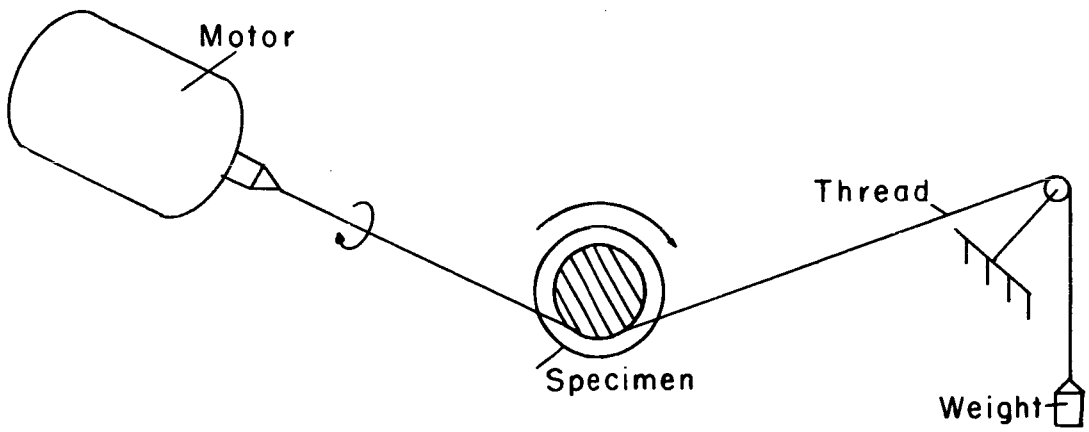

Figure 3.- Polishing technique. Notched specimens.

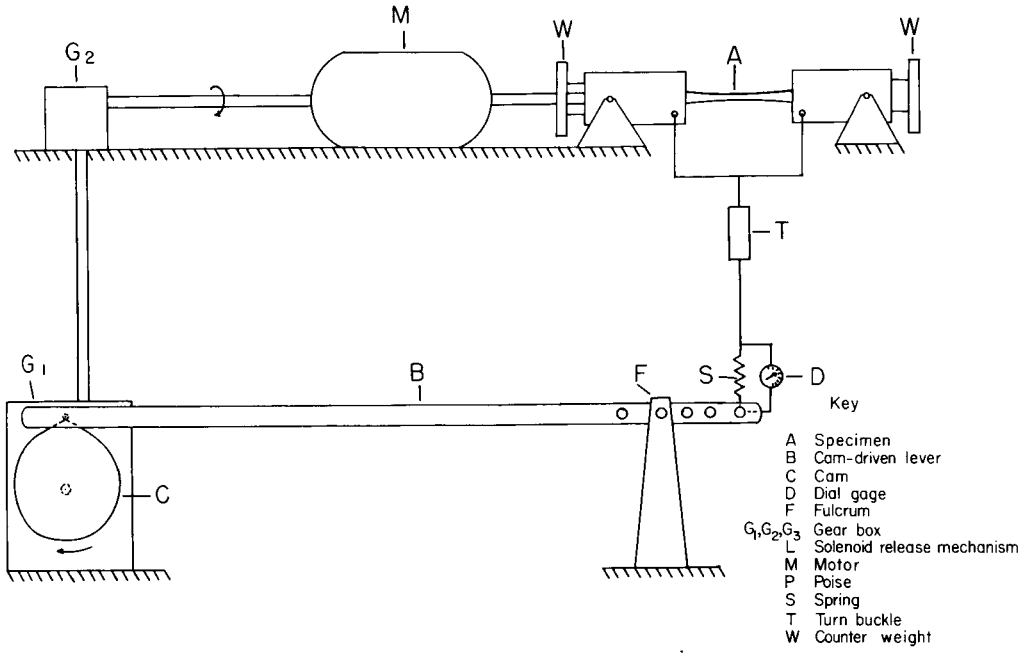

(a) Sinusoidal and exponential spectrum.

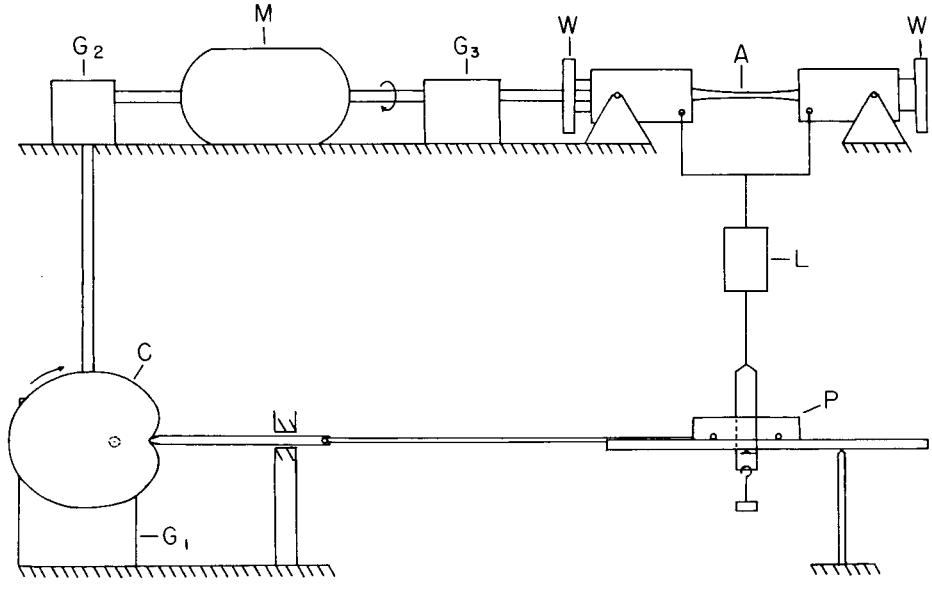

(b) Gust-frequency spectrum.

Figure 4.- Variable-amplitude loading devices.

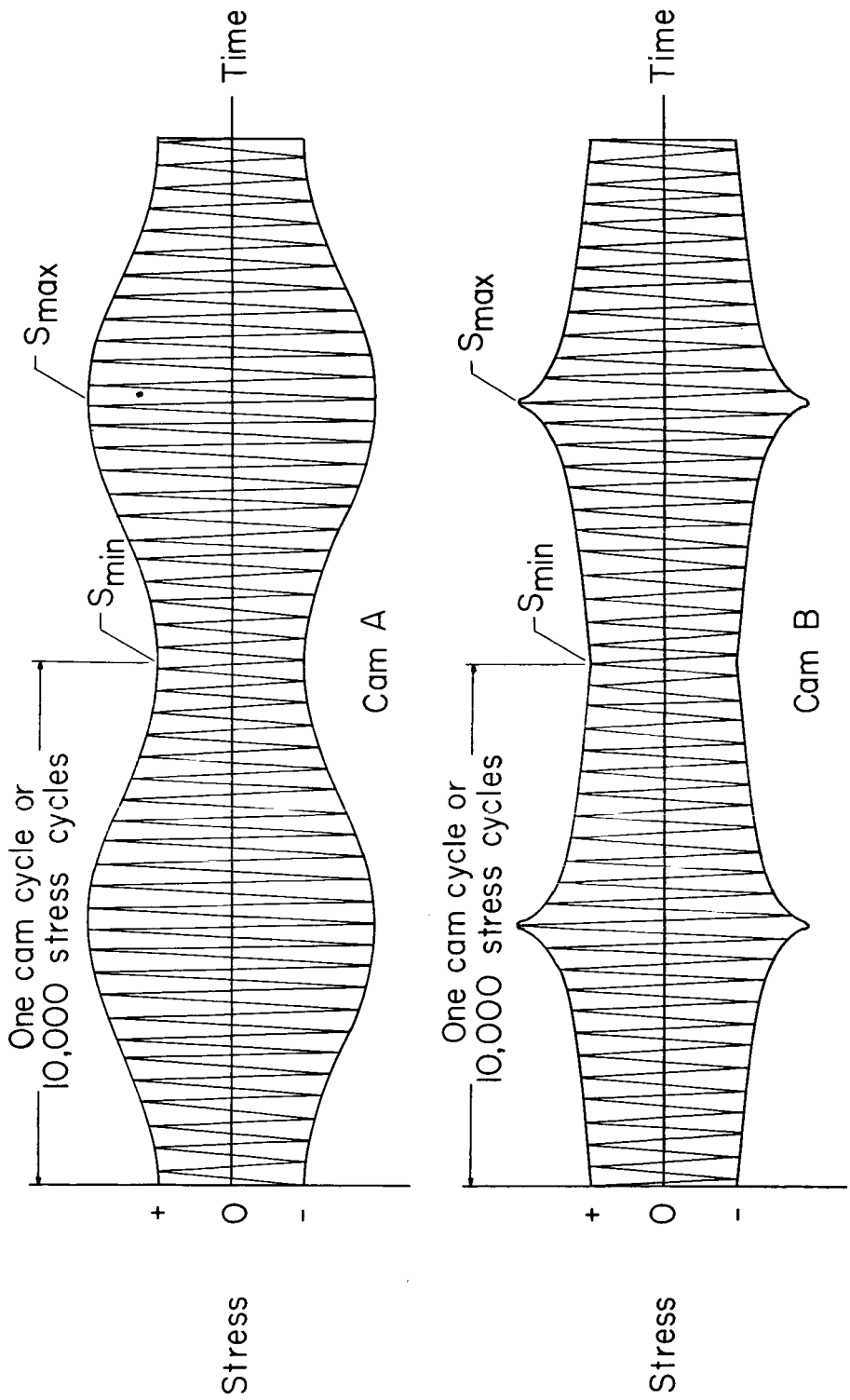

Figure 5.- Stress histories.

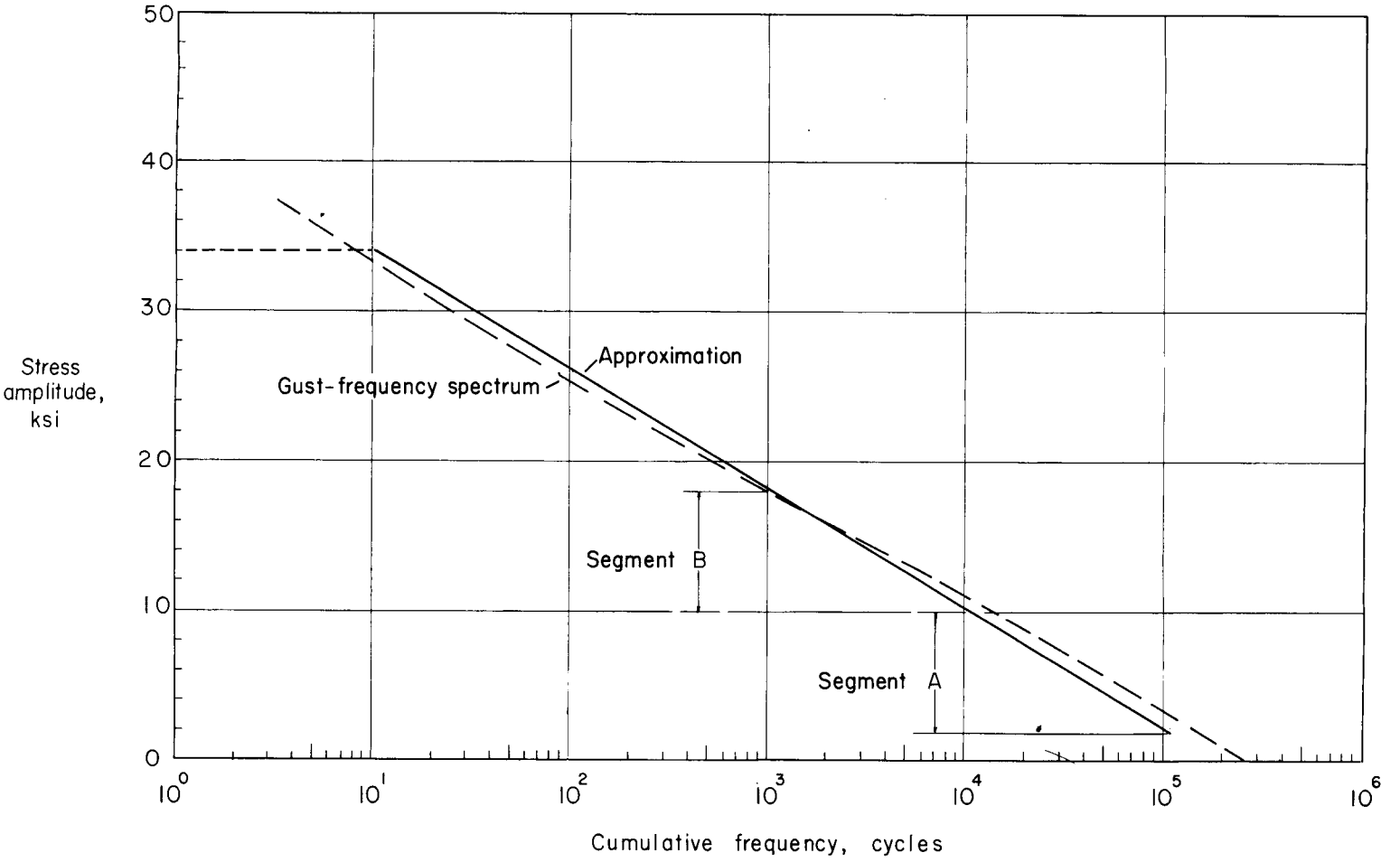

Figure 6.- Approximation of gust-frequency spectrum by segments.

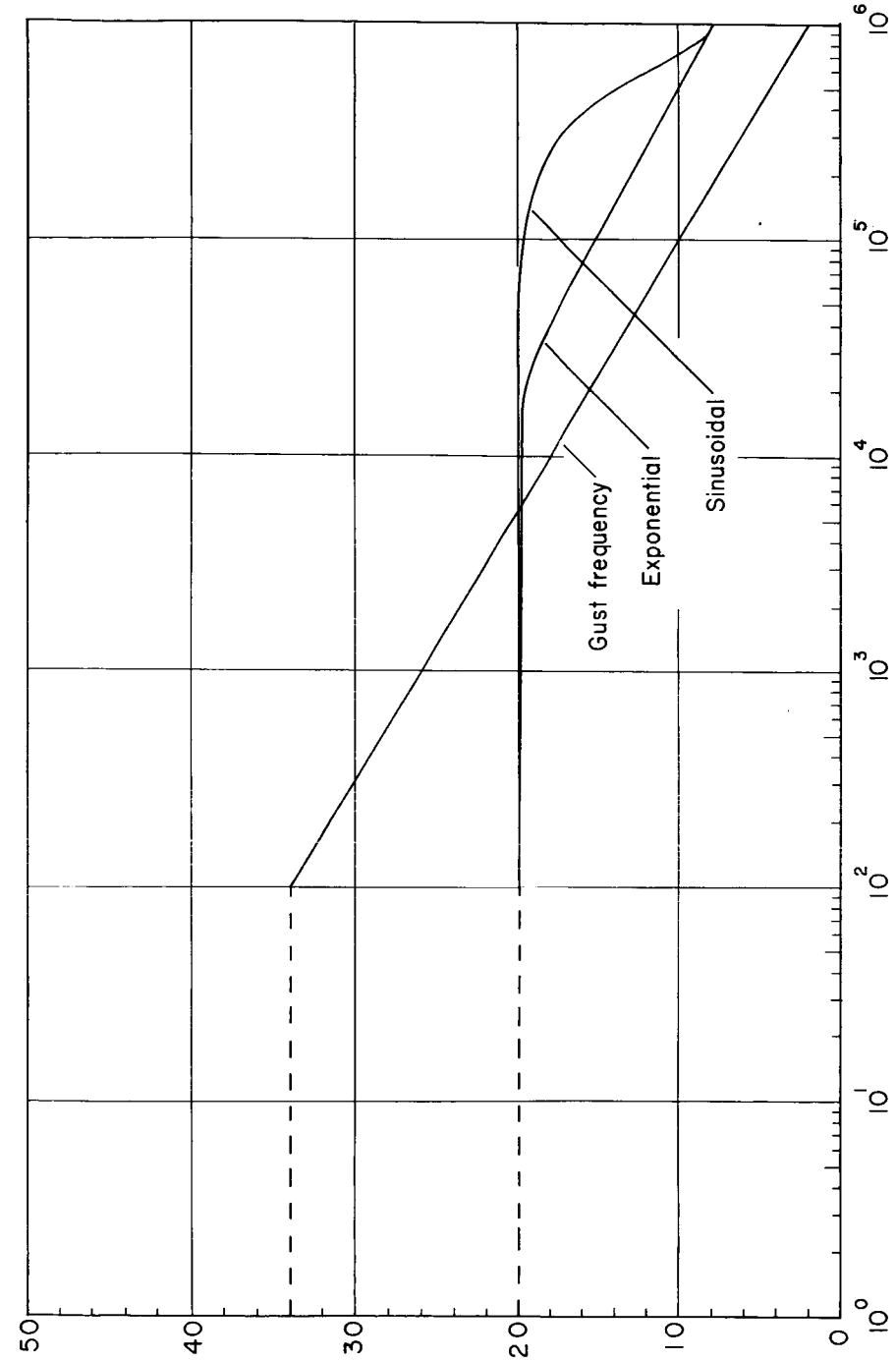

Figure 7.- Comparison of cumulative frequency curves for 10^4 cycles of each of the test spectra used.

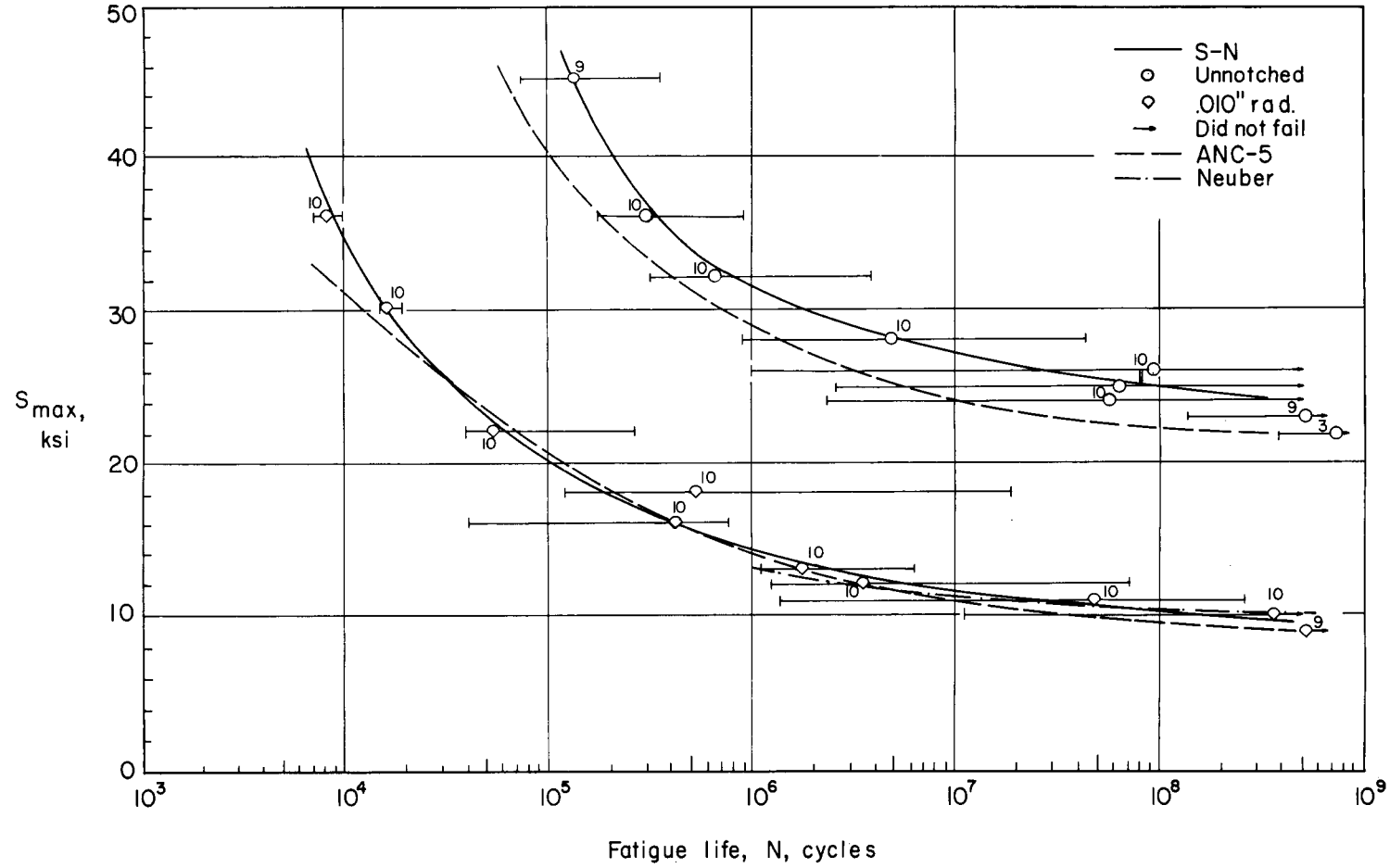

Figure 8.- Results of constant-level tests of unnotched specimens and specimens with 0.010-inch notch radius. Numbers refer to number of specimens tested and ticks indicate range of data for each test condition.

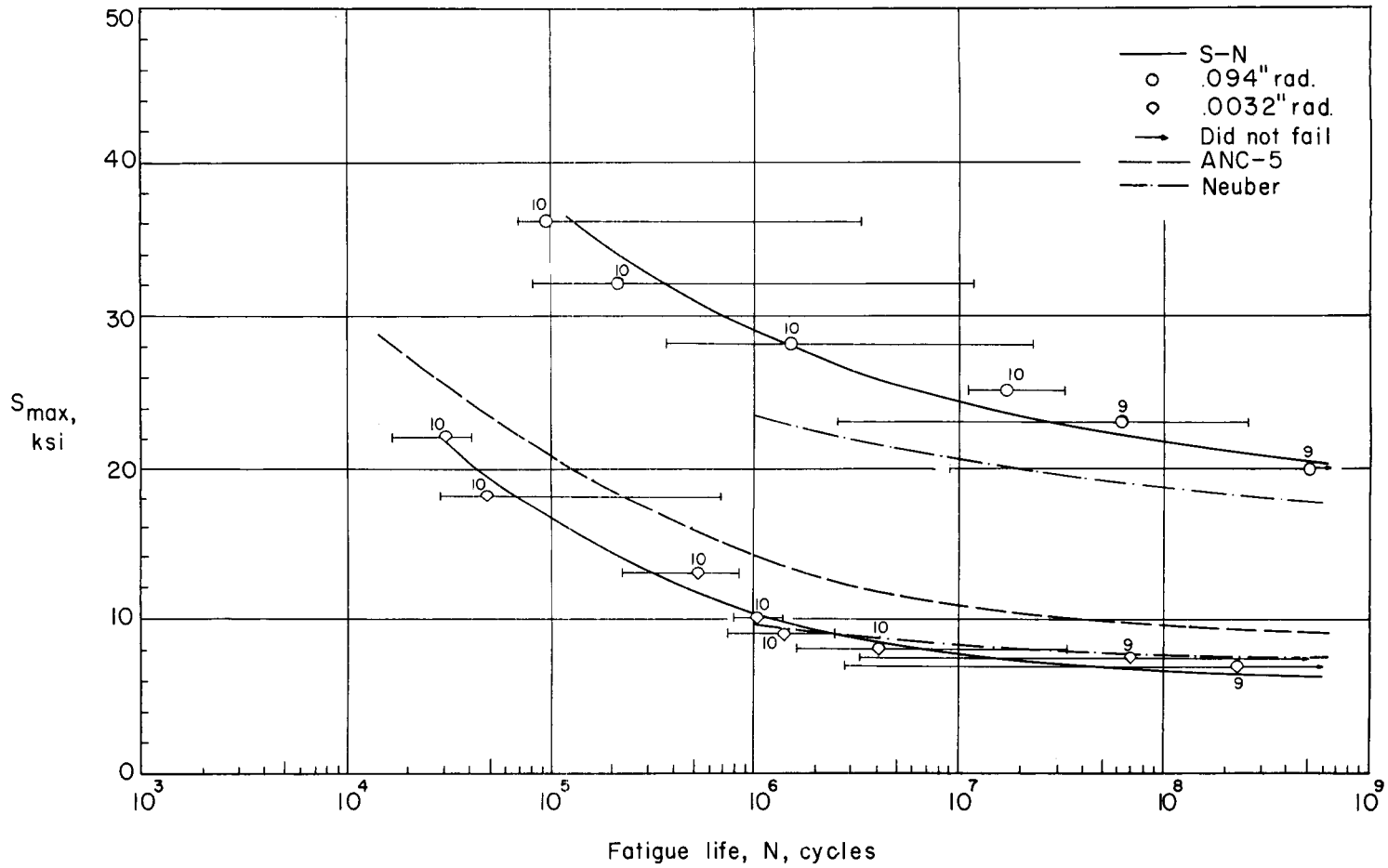

Figure 9.- Results of constant-level tests of unnotched specimens and specimens with 0.094-inch and 0.0032-inch notch radius. Numbers refer to number of specimens tested and ticks indicate range of data for each test condition.

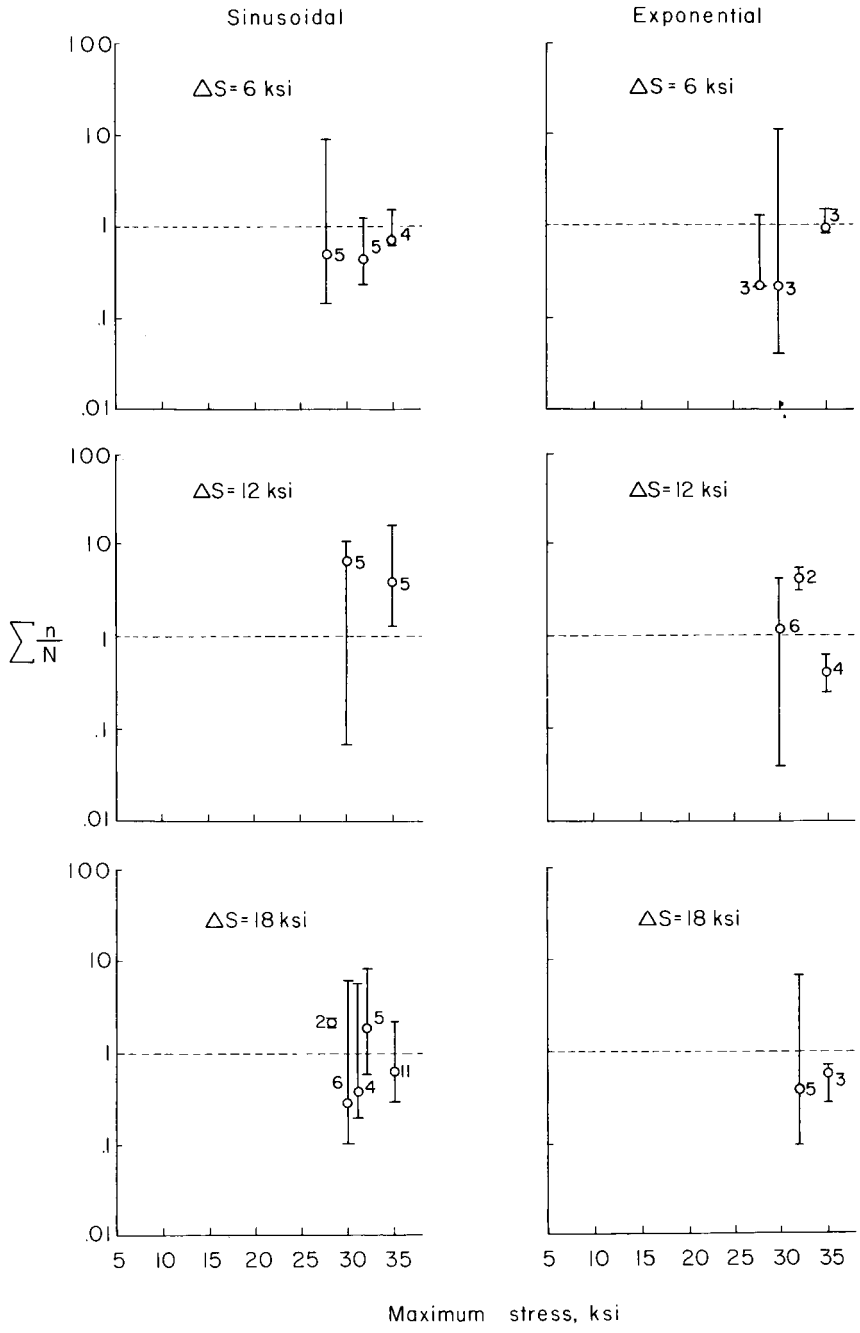

Figure 10.- Results of variable-amplitude tests. Unnotched specimens; sinusoidal and exponential spectra. Numbers refer to number of specimens tested and ticks indicate range of data for each test condition.

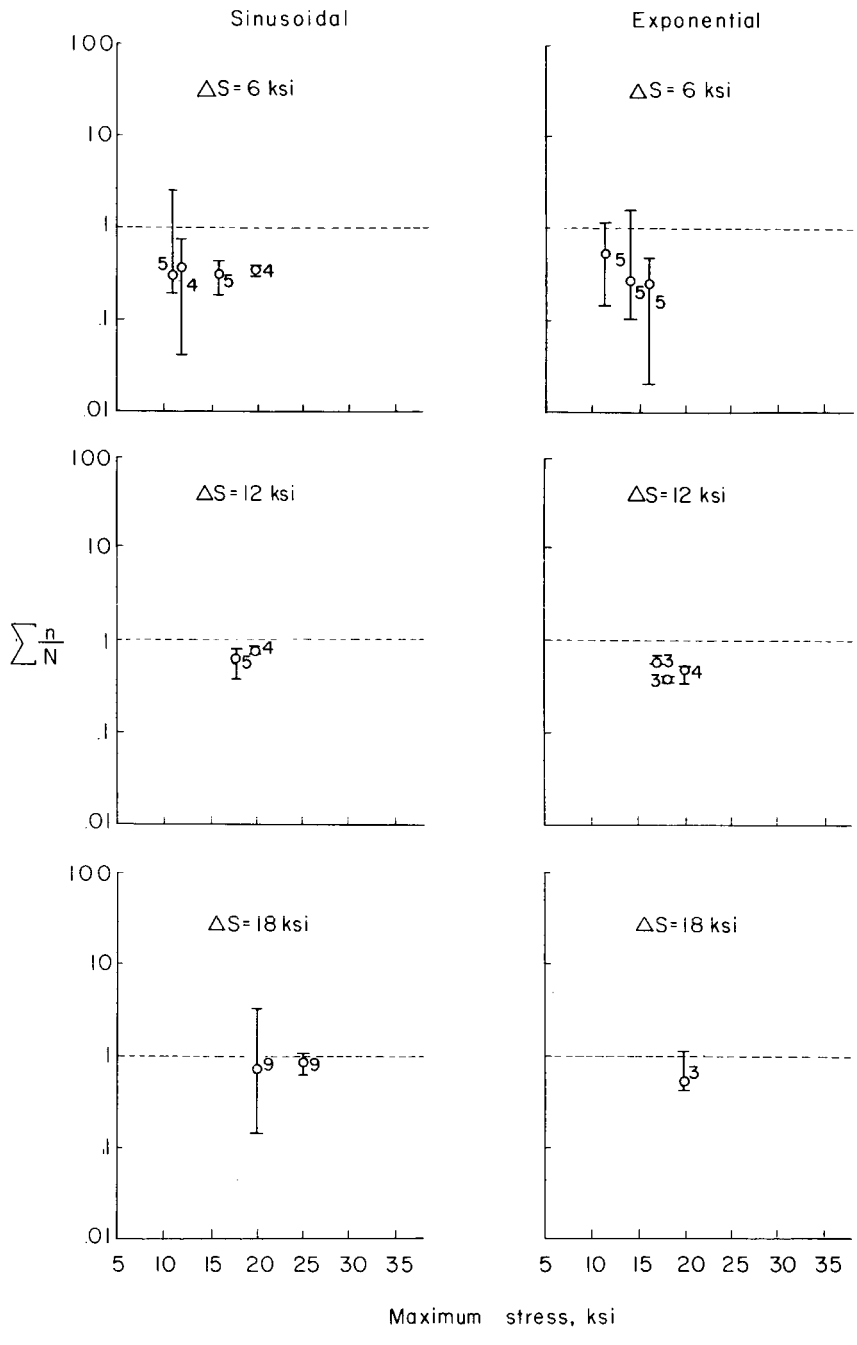

Figure 11.- Results of variable-amplitude tests. Specimens with 0.010-inch radius notch; sinusoidal and exponential spectra. Numbers refer to the number of specimens tested and ticks indicate range of data for each test condition.

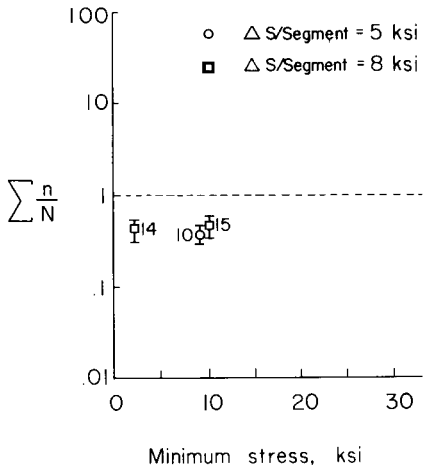

Figure 12.- Results of variable-amplitude tests. Specimens with 0.010-inch radius notch; simulated and modified gust-frequency spectrum. Numbers refer to the number of specimens tested and ticks indicate the range of data for each test condition.